Hindawi
International Journal of Polymer Science
Volume 2023, Article ID 5591108, 20 pages
https://doi.org/10.1155/2023/5591108

Research Article

Effect of *Raphia vinifera* Fibre Size and Reinforcement Ratio on the Physical and Mechanical Properties of an Epoxy Matrix Composite: Micromechanical Modelling and Weibull Analysis

Syrille Brice Tchinwoussi Youbi,[1,2] **Omar Harzallah**,[3] **Nicodème Rodrigue Sikame Tagne**,[1,2,4,5] **Paul William Mejouyo Huisken**,[1,2] **Tido Tiwa Stanislas**,[4,6] **Jean-Yves Drean**,[3] **Sophie Bistac**,[7] **and Ebenezer Njeugna**[1,2]

[1]*Mechanics and Adapted Materials Laboratory (LAMMA), ENSET—University of Douala, Cameroon*
[2]*Mechanics Laboratory (LM), ENSET—University of Douala, Cameroon*
[3]*Université de Haute-Alsace, LPMT UR 4365, F-68100 Mulhouse, France*
[4]*Research Unit in Engineering of Industrial Systems and the Environment (UR-2MSP), IUT/FV Bandjoun—University of Dschang, Cameroon*
[5]*Research Unit in Mechanics and Modelling of Physical Systems (UR-2MSP), Faculty of Science—University of Dschang, Cameroon*
[6]*Laboratoire COVACHIM-M2E, EA3592, UFR SEN, Université des Antilles, Campus de Fouillole, BP 250 97157 Pointe-à-Pitre, Guadeloupe, France*
[7]*Laboratoire de Photochimie et d'Ingénierie Macromoléculaires, Université de Haute Alsace, 3b rue Alfred Werner, Mulhouse Cedex, France*

Correspondence should be addressed to Syrille Brice Tchinwoussi Youbi; youbicyrille@gmail.com

Received 20 January 2023; Revised 18 April 2023; Accepted 10 May 2023; Published 23 May 2023

Academic Editor: Chenggao Li

Copyright © 2023 Syrille Brice Tchinwoussi Youbi et al. This is an open access article distributed under the Creative Commons Attribution License, which permits unrestricted use, distribution, and reproduction in any medium, provided the original work is properly cited.

This study evaluates the effects of lengths and reinforcement ratio of *Raphia vinifera* fibres (RVFs) on the physical and mechanical properties of an epoxy matrix composite. Three volume fractions (20%, 30%, and 40%) and three lengths (5, 10, and 15 mm) of fibres were used to produce the composite, and the samples were subjected to the absolute and apparent density, porosity, water absorption rate, and tensile and flexural strength. The probability of failure of the composite is described by the means of two-factor Weibull model. In addition, a theoretical approach to predict mechanical characteristics based on empirical models was carried out. The results show that the addition of RVF decreases the density of the composite, while the porosity and absorption rate increase. The mechanical test shows that the tensile and flexural stress and Young's modulus of the composite are lowered compared to those of the resin alone. Multivariate analysis of variance (MANOVA) and Tukey test showed that fibre lengths and reinforcement ratio significantly lower the mechanical properties of the composite. The distribution of strength and Young's modulus follows Weibull's law. Furthermore, the Cox–Krenkel mathematical model has the best approximated model for the experimental results after the tensile test. Based on these results, this material could be used as reinforcement parts for vehicle backrests or interior decoration in the construction industry.

1. Introduction

The environmental constraints linked to the production of "green" materials are leading to the search for alternatives to conventional synthetic materials such as carbon and glass [1], which are not only non-biodegradable but whose production generates large emissions of polluting gases [2]. Although highly criticised for their high hydrophilicity [3], natural fibres offer an alternative for the elaboration of new bio-composites that are more respectful of the environment because they are biodegradable [5], low density, and can be easily functionalized [6]. Plant fibres, such as sisal,

hemp, and kenaf, are commonly used as reinforcements in the manufacture of composites for industrial use (automotive, aerospace, and construction) [7], with different forming methods (contact moulding, injection moulding) [8]. Several studies show that the mechanical properties of short fibre composites are sensitive to the lengths and volume fraction of the fibres in the composite. These properties tend to decrease when the fibre lengths exceed 30 mm [9] and the volume fraction 40% [10]. As the demand for bio-composites with plant fibre reinforcements is increasing [7], the development of a predictive model to characterise (mechanical, physical) a material without having to resort to experimentation can save time and costs by making composites more accessible [11]. Among the methods for predicting the characteristics of short fibres composites is mathematical homogenisation [12], which is achieved by empirical models such as the law of mixtures [13], Halpin–Tsai (HT) [14], Cox–Krenkel [15], or Kelly and Tyson models [16], which allow the analytical prediction of the mechanical behaviour of composites, saving considerable time in the process of popularising bio-composites [17]. Among the methods of all the statistical analysis methods, only the weibull method [18], offers the particularity of providing information on the severity of the factors inducing the failure of the composite while predicting its mechanical behaviour [19].

Among natural fibres, *Raphia vinifera* (RV) is abundant in tropical regions and is not widely used in composites [20]. The RV from which the fibres originate is generally found in the Amazon, tropical Africa, and Madagascar [21]. RV is generally used for decorative objects (chairs, tables) [22] and as raw material for the textile industry [23]. Several studies have been carried out on *Raphia vinifera* fibres (RVFs) from the stem to determine its mechanical and physical properties for potential application in composites [24]. This work has shown that RVF can be used for the development of bio-composites [17] and the production of cellulose [25]. Work on the development of composites reinforced with RVF from sheets has shown that the addition of short, random fibres reduces the mechanical properties (modulus and strength) of the polyester matrix [26]. The use of RVF from the stem as a reinforcement of composite materials with regards to properties is therefore of great interest for the development of bio-composites [23, 24]. Natural fibres, such as basalt [27], cotton [28], bamboo [29], flax [30], and coir [31], have surface energy favouring their use as reinforcements for the development of epoxy matrix biocomposites with appreciable results from the mechanical and interfacial point of view, for those reinforced with bamboo fibres [2], basalt fibres [32], flax fibres [33], coconut fibres [34], and cotton fibres [35], thus representing a major interest for the industry [11, 36]. In addition, a previous study by Youbi et al. [37] on the wettability of RVF from the stem shows good surface energy, making this fibre interesting for the development of an epoxy matrix biocomposite. To the best of our knowledge, there are no works in the literature review in which short, random fibres of RV from the stem are used in the reinforcement of epoxy matrix composites.

Based on the literature, RVF offers good mechanical properties to be used in the composite, the cavities inside the fibre contribute to making it very light and therefore the composite to be made, and the abundant availability of its fibres. In addition, recent work has demonstrated its good adhesion properties with matrices such as epoxy. Previous studies on raffia fibres in composite materials are limited to the use of long, woven fibres as reinforcement. An isotropic epoxy matrix composite reinforced with short random RVF fibres was produced to evaluate its physical, mechanical and micromechanical behaviour. The present work contributes to the valorisation of RVF for the development of new "green" composite materials that are more environmentally friendly. The objective of this work is to produce and characterise epoxy composites reinforced with short random fibres from VR and to predict their behaviour. To this end, the physical and mechanical properties were evaluated, and a statistical analysis of the mode of failure was carried out using the Weibull method as well as a mathematical homogenisation in order to predict the mechanical behaviour of the composite in tension.

2. Materials and Methods

2.1. Tested Materials. The RV used is harvested in the lowlands of the Western Region of Cameroon, in the Hauts-Plateaux sub-division, is about 10 years old, and the time elapsed between harvest and use is 30 days. The fibres were mechanically extracted according to the method described by Njeugna et al. [24] and then dried for 24 hours at a temperature of 105°C as recommended by Baley et al. [38] and Espinach et al. [39] with vegetal fibres. Nine formulations were made based on combinations of three fibre lengths (5, 10, and 15 mm) [26] and three-volume fractions (20%, 30%, and 40%). To prepare the fibres, approximately eight fibres of 300 mm length were first grouped into batches, measured with a mm ruler, and marked to ensure uniformity of length. The chisel was then used to cut the fibres to lengths of 5, 10, and 15 mm. The epoxy resin used was supplied by a local structure "SUPER MESURE" in Cameroon and according to it, the epoxy resin is Polypox (100% purity) of the diglycidyl ether type of bisphenol A (DGEBA) from Germany, and an aromatic diamine from Switzerland was used as a curing agent. Mixing (fibre, resin, and hardener) is carried out in a 1000 W mini-mixer, to ensure the homogeneity of the composite [40] for 5 minutes at an ambient temperature of 30 ± 2°C. The moulded samples were then cured for 5 hours at room temperature. These formulations are coded as EP-RVF *X*–*Y* with EP for epoxy, RVF for *Raphia vinifera* fibres, *X* the volume fraction of the fibres in the composite, and *Y* the lengths of the RVF. The EP-RVF 0 formulation is the matrix formulation alone. Table 1 shows all the formulations made for the present work.

The difficulty of measuring fibre (ϑ_f) and matrix (ϑ_m) volume fractions in practice needs the calculation of matrix and fibre mass fractions (m_m and m_f) given by Equation

Table 1: Designation of the combinations according to the lengths and volume fraction of the fibres.

Formulations	EP-RVF 0	EP-RVF 20			EP-RVF 30			EP-RVF 40		
RVF (%)	0	20			30			40		
Lengths (mm)	0	5	10	15	5	10	15	5	10	15

(1) and used by Huisken et al. [41] in the development of palm nut mesocarp fibre composites

$$\begin{cases} m_m = \dfrac{\rho_m}{\rho_{f\times\vartheta_f} + \rho_m(1-\vartheta_f)}\vartheta_m \\ m_f = \dfrac{\rho_f}{\rho_{f\times\vartheta_f} + \rho_m(1-\vartheta_f)}\vartheta_f \end{cases}, \quad (1)$$

with ϑ_m and ϑ_f, respectively, are the volume fraction of the fibre and matrix, ρ_f and ρ_m are the density of the fibre and matrix, $\rho_m = 1200\,kg/m^3$ [42], and $\rho_f = 180\,kg/m^3$ [23].

The samples were made by contact moulding [8] to preserve the cavities in the RVF highlighted by Tagne et al. [23]. Figure 1 shows the method of obtaining the samples used for the mechanical and physical characterisations.

2.2. Physical Characterisation of the EP-RVF

2.2.1. Bulk and Real Density. The bulk density was determined by the gravimetric method by ASTM D 792-07 [43]. 15 specimens are selected for fibre length and fibre volume fraction, i.e., a total of 150 specimens for all formulations, with dimensions of $15\,mm \times 15\,mm \times 15\,mm$ were tested, and the mass of the samples was determined using an ADAM brand balance with a precision of 10^3 g. The bulk density was determined using Equation (2).

The true density was determined by the gravimetric water column displacement method according to ASTM D 2734-03 [44], and 15 specimens are also selected for fibre length and fibre volume fraction, i.e., a total of 150 specimens for all formulations were made waterproof by paraffin coating. The true density was determined through Equation (3):

$$\rho_a = \frac{m_c}{V_c}, \quad (2)$$

$$\rho_r = \frac{m}{V_{rc}}, \quad (3)$$

with ρ_a the apparent density of the composite ($kg\,m^{-3}$), m_c the mass of the composite (kg), V_c the apparent volume of the composite (m^3), ρ_r real density ($kg\,m^{-3}$), m the mass of the sample before immersion (kg), and V_{rc} the difference between the initial volume of water and the maximum volume (m^3).

2.2.2. Porosity Rate. The porosity rate was determined in accordance with ASTM D 2734-03 [44]. The porosity rate p (%) was determined by Equation (4) and used by other authors for the evaluation of the porosity of palm kernel mesocarp fibre-reinforced composites [41]

$$p(\%) = \frac{(\rho_r - \rho_a)}{\rho_r} \times 100. \quad (4)$$

2.2.3. Water Absorption Rate. The water absorption rate was obtained according to ASTM D 570-85 [45], and 15 specimens are selected for one fibre length and one fibre volume fraction, i.e., a total of 150 specimens for all formulations. The pre-weighed samples were immersed in distilled water and then weighed until a constant mass was obtained [41]. The absorption rate was determined by Equation (5):

$$W(\%) = \frac{(Ws - W_0)}{W_0} \times 100, \quad (5)$$

with W (%) the absorption rate, W_S the mass of the sample at saturation (kg), and W_0 the initial mass of the sample (kg).

2.3. Mechanical Characterisation of the EP-RVF in Tension.

The tensile tests were carried out according to ASTM D 638-14 [46], as described by Mohana et al. [47] and Hassan et al. [48]. The dimensions of the specimens were $115\,mm \times 10\,mm \times 9\,mm$, and 10 specimens are selected for one fibre length and one fibre volume fraction, i.e., a total of 100 specimens for all formulations were tested. The tensile test was carried out on an MTS 20/M tensile testing machine with a test speed of 5 mm/min and a load cell of 20 kN, the distance between jaws being 105 mm. The tensile strength and Young's modulus in tension were determined by Equations (6) and (7) [41, 49]:

$$\sigma_t = \frac{F_t}{h \times l}, \quad (6)$$

$$E_t = \frac{\sigma_t}{\varepsilon}, \quad (7)$$

where σ_t is the tensile strength (MPa), F_t is the tensile breaking force (N), h and l, respectively, are the height and length of the specimen section (mm), ε is the strain, and E_t is the Young's modulus (MPa).

The determination of E_t is done from the slope of the linear zone of the curve $\sigma_t = f(\varepsilon)$. This approach has been used in other work [50].

2.4. Mechanical Characterisation of EP-RVF in Three-Point Bending.

The specimens and three-point bending tests were performed according to ASTM D 790-03 [51], as described by Jeyapragash et al. [5] and Mehra et al. [52]. 10 specimens are selected for a fibre length and fibre volume fraction, i.e., a total of 100 specimens for all formulations and of dimensions $115\,mm \times 10\,mm \times 9\,mm$ were tested on an universal tensile test machine (MTS 20/M) with a test speed of 5 mm/min and a load cell of 20 kN, the distance between supports being 90 mm. The flexural strength and Young's

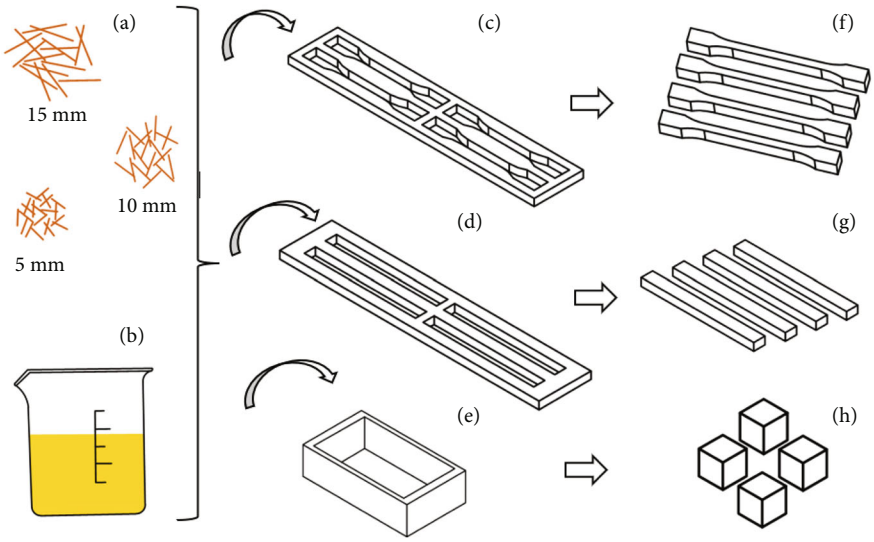


Figure 1: Obtaining of samples: (a) RVF lengths, (b) epoxy resin and RVF mixing jar, (c) tensile sample moulds, (d) flexural sample mould, (e) physical characterisation sample mould, (f) tensile samples, (g) flexural samples, and (h) physical characterisation samples.

modulus in bending were determined by Equations (8) and (9) and used by other authors in the characterisation of plant fibre composites [41, 49]

$$\sigma_f = \frac{3 \times F_f \times L}{2 \times l \times h^2}, \tag{8}$$

$$E_f = \frac{L^3}{4 \times l \times h^3}\left(\frac{\Delta F_f}{\Delta f}\right), \tag{9}$$

where F_f is the bending force (N), f is the displacement induced by the force (mm), the ratio $(\Delta F_f)/\Delta f$ is taken in the linear area of the bending curve, L is the length between supports (mm), l and h, respectively, are the thickness and height of the sample section (mm).

2.5. Statistical Analysis

2.5.1. Multivariate Analysis of Variance. Multivariate analysis of variance (MANOVA) and Tukey's test were carried out to assess the impact of independent factors (fibre lengths and volume fraction) on the dependent responses (tensile and bending stress and modulus) using SPSS-21 software. The confidence level was set at 90%, and the null hypothesis was formulated as follows: lengths and volume fractions have no effect on the mechanical behaviour of the composite. The MANOVA method has also been used for statistical optimisation of composite materials [53–55].

2.5.2. Weibull Analysis. Weibull analysis is particularly useful when the test results show considerable dispersion [56]. When the distribution of the results of a mechanical test does not follow the Weibull distribution, then its failure is due to the presence of structural defects. In the case where the distribution of results follows the Weibull analysis, the observed failure is only due to the stress on the material. For this second use, the failure or survival of the samples can be predicted [57].

The two-factor Weibull statistical distribution has advantages such as its ability to be expressed as a function, which makes it an easy tool to apply [58]. In addition, the two-factor Weibull distribution describes with high accuracy the probability of failure of composites [59]. The density function of the two-parameter Weibull distribution is given by Equation (10) [59–61]. The cumulative failure probability is given by Equation (11) and is obtained by integrating the density function [60].

The Weibull parameter (m) is used to assess the distribution of structural defects in the material: when $m < 20$, then the brittle failure of the material is due to the stress on the material [62]. This parameter m is deduced from the graphical solution of Equation (12) considered as an equation of the type $Y = mx + 1$ with $Y = \ln(-\ln(1 - P_r))$, $mx = m \ln(\sigma)$, $b = m \ln(\sigma_0)$ [63]. The probability of failure P_r can be estimated using either the median rank or Bernard approximation (Equation (13)), the mean rank or Herd–Johnson approximation (Equation (14)), or the modified Kaplan–Meier approximation, also called the Hazen approximation (Equation (15)) [64]. In order to assert whether the distribution follows a Weibull distribution or not, the linear correlation coefficient R^2 is used. Doremus [65] show that a distribution follows a Weibull distribution when $R^2 > 0.95$, and the authors also state that it does not follow a Weibull distribution for $R^2 < 0.90$; but when the correlation coefficient is in the interval [0.90–0.95], we cannot conclude directly. It is therefore necessary to calculate the Anderson–Darling surplus value (p): the distribution follows a Weibull distribution when $p > 0.05$ [66].

$$f(x) = \frac{\beta}{\alpha}\left(\frac{x}{\alpha}\right)^{\beta-1} e^{\left(\frac{x}{\alpha}\right)^{\beta}}, \tag{10}$$

$$f(x) = 1 - e^{\left(\frac{x}{\alpha}\right)^{\beta}}, \tag{11}$$

$$\ln(-\ln(1 - P_r)) = m \ln(\sigma) - m \ln(\sigma_0), \tag{12}$$

$$P_r = \frac{i - 0.3}{n + 0.4}, \quad (13)$$

$$P_r = \frac{i}{n + 1}, \quad (14)$$

$$P_r = \frac{i - 0.5}{n}, \quad (15)$$

with $f(x)$ is the two-parameter Weibull distribution density; β is the shape parameter of the distribution ($\beta = m$), x is the independent variable (consecutively the tensile and bending stress for the present work), α is the shape parameter of the distribution, p_r is the probability of failure, m is the Weibull parameter, σ is the experimental stress, and σ_0 is the normalisation stress (MPa).

2.6. Mathematical Homogenisation. The mathematical homogenisation was focused on the tensile mechanical properties of the composites due to the already known tensile properties of EP-RVF [23].

The HT model was developed for the purpose of characterising long and continuous fibre-reinforced composites [67] and used by Espinach et al. [39] and Migneault et al. [16]. The original model was modified by Nielsen to suit short random fibre composites [68]. The Young's modulus by the modified HT method is derived from Equation (16) [12, 15]:

$$E_{TH} = E_m \left(\frac{1 + \xi \times \eta \times V_f}{1 - \eta \times \psi \times V_f} \right), \quad (16)$$

where E_{TH} is the theoretical modulus of the modified HT composite, E_m is the modulus of the matrix (MPa), V_f is the volume fraction of the fibre, ξ is the parameter on which the fibre geometry depends ($\xi = 2.8$) [12], ψ is a factor depending on the fibre geometry and is determined by Equation (17) and η is expressed by Equation (18), φ_{max} is the maximum fibre packing fraction ($\varphi_{max} = 0.52$) [12]. The theoretical stress is determined by replacing the Young's modulus with the strength in Equations (16) and (18):

$$\psi = 1 - \left(\frac{1 - \varphi_{max}}{\varphi_{max}^2} \right) V_f, \quad (17)$$

$$\eta = \frac{E_f/E_m - 1}{E_f/E_m + \xi}. \quad (18)$$

The Cox–Krenkel model is an improvement of the Cox model for application to random short fibre-reinforced composites, which is a variant of the law of mixtures [15] and has been used by Vilaseca et al. [13] for the prediction of the characteristics of a hemp fibre composite reinforcing a polypropylene matrix. The modulus is obtained by Equation (19). The theoretical stress is determined by replacing the Young's modulus with the stress in Equation (19):

$$E_{TC} = \eta_0 \times \eta_1 \times E_f \times V_f + E_m(1 - V_f), \quad (19)$$

where η_0 is the fibre orientation factor. For a random distribution, $\eta = \eta_1$, E_{TC} the theoretical Cox–Krenkel Young's modulus (MPa).

The Kelly and Tyson model is an improvement of the Cox–Krenkel model and is intended to be more accurate [15]. It will therefore be tested whether it approaches the experimental results better than the Cox–Krenkel model. The stress and modulus are determined by Equations (20) and (21):

$$\sigma_{TK} = \eta_0 \times \eta_{ls} \times \sigma_f + \sigma_m(1 - V_f), \quad (20)$$

$$E_{TK} = \eta_0 \times \eta_{lE} \times E_f \times V_f + Em(1 - V_f), \quad (21)$$

where η_{lS} and η_{lE}, respectively, are the fibre efficiency factor for the composite in tension and bending, σ_{TK} and E_{TK}, respectively, are the Kelly and Tyson theoretical stress and Young's modulus (MPa). The critical fibre length is the ratio of the tensile stress and the fibre radius to the interfacial shear stress, as presented by Equation (22). Experimental measurement of the critical fibre length and interfacial shear stress is difficult to achieve and may assume that there is good adhesion between the fibre and the matrix. However, the shear stress can be related to the tensile stress by Equation (23) [15]:

$$l_c = \frac{\sigma_f \times r}{\tau}, \quad (22)$$

$$\tau = 3^{-1/2} \times \sigma_m, \quad (23)$$

where l_c is the critical length of the fibre (mm), σ_f is the tensile strength (MPa), r is the radius of the fibre (mm), τ is the shear stress between the fibre and the matrix, and σ_m is the tensile strength of the matrix (MPa).

The fibre efficiency factor for determining the theoretical tensile strength is defined by Equation (24) for $l > l_c$ and Equation (25) for $l > l_c$. While the fibre efficiency factor for the determination of the tensile Young's modulus is given by Equation (26),

$$\eta_{ls} = 1 - \frac{S_c}{2S}, \quad (24)$$

$$\eta_{ls} = \frac{S}{2S_c}, \quad (25)$$

$$\eta_{lE} = \frac{1 - \tanh\ (\beta \times S)}{\beta \times S}, \quad (26)$$

$S = l/d$ is the aspect ratio of the fibre, $S_c = l_c/d$ is the critical factor of the fibre, h is the height of the specimen, β is a factor defined by Equation (27), G_m is the transverse modulus of elasticity of the matrix (MPa), r is the radius of the fibre, and R is the centre-to-centre distance defined by Equation (28).

$$\beta = \left(\frac{2 \times G_m}{E_f \times \ln\left(\frac{R}{r}\right)} \right)^{1/2}, \quad (27)$$

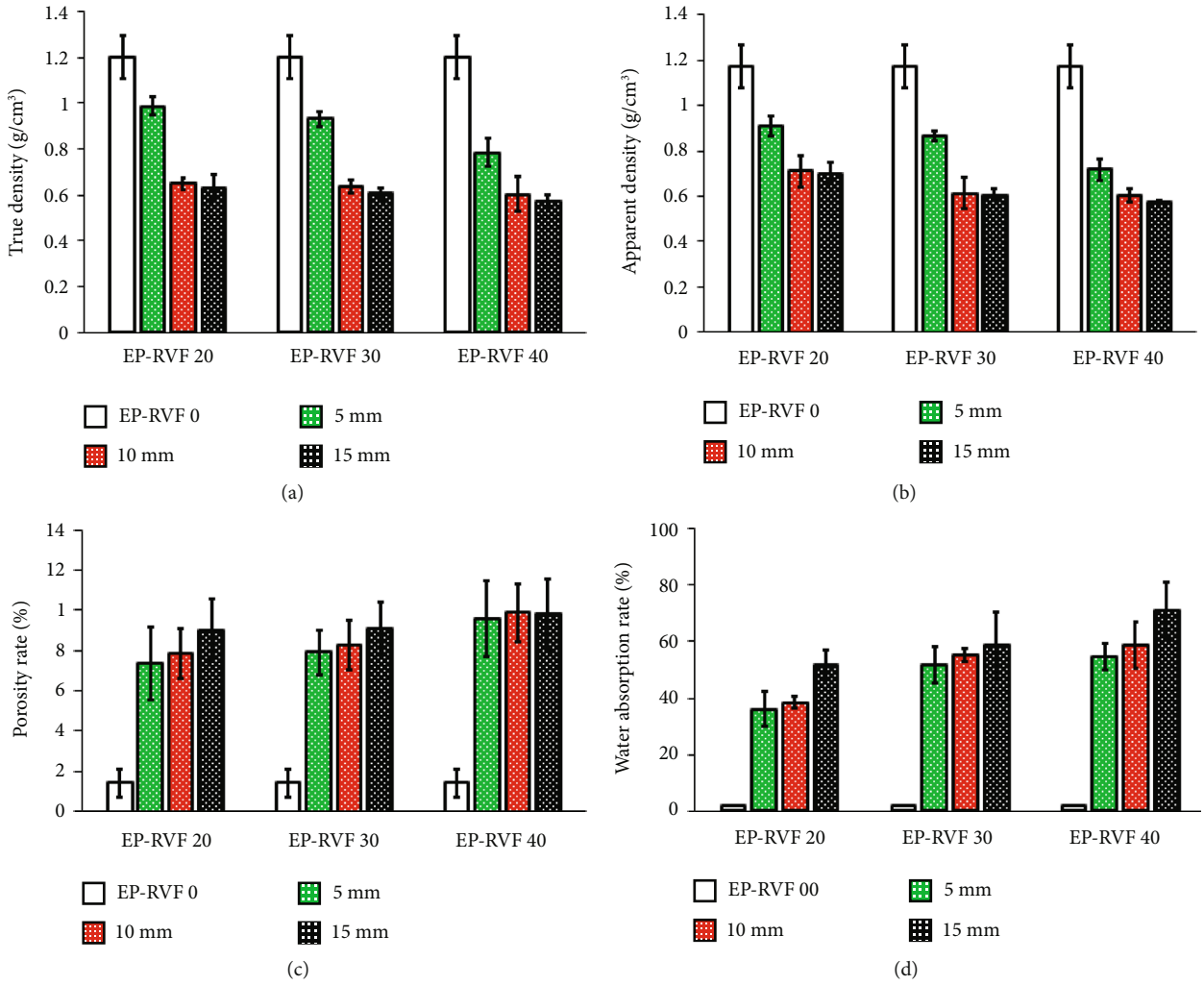


Figure 2: Physical properties of EP-RVF composites: (a) bulk density, (b) true density, (c) porosity rate, and (d) absorption rate.

$$R = r\left(\frac{\pi}{4 \times V_f}\right)^{1/2}. \quad (28)$$

3. Results and Discussion

3.1. Real and Bulk Densities, Porosity, and Water Absorption Rate of EP-RVF. Figures 2(a) and 2(b) show the results of the bulk and true density of the EP-RVF composite, respectively. Both the bulk and true densities show that increasing the fibre volume fraction in the composite decreases the densities. Figure 2(a) shows that for all fibre lengths, the minimum value of bulk density is observed for the EP-RVF 40 samples with a reduction of 34.60%, 49.58%, and 52.12%, respectively, for the fibre lengths of 5, 10, and 15 mm compared to the EP-RVF 0 samples. Similar facts are observed for the real density represented in Figure 2(b) with decreases of 38.87%, 48.38%, and 50.88%, respectively, for the fibre lengths of 5, 10, and 15 mm compared to the EP-RVF 0 samples. This phenomenon of decreasing density with increasing reinforcement ratio and lengths has also been observed in palm nut mesocarp fibre composites [41] and could be attributed to the fact that the density of RVF is lower [23] than that of epoxy resin [42]. In addition, the increase in fibre volume fraction from 20% to 40% also decreases the bulk density of the composite by 35.84%, 34.90%, and 26.78%, respectively, for the 20%, 30%, and 40% fibres, while the decrease in actual density is estimated at 22.94%, 29.84%, and 19.64%, respectively, for the 20%, 30%, and 40% fibres for the same lengths and formulations. This can be attributed to the low density of the RVF [23] and its porous character [24].

Figure 2(c) shows that the porosity increases with lengths and fibre volume fraction in the EP-RVF composite. This increase in porosity for the 20%, 30%, and 40% of fibres, respectively, is estimated to be 84.86%, 85.34%, and 85.26% compared to the EP-RVF 0 samples. However, increasing the length of the fibres between 5 and 15 mm also increases the porosity by 22.37%, 15.20%, and 2.68% for the 5, 10, and 15 mm fibre lengths, respectively. This high porosity could be attributed to cavities in the RVF [24, 69], to the presence of bubbles in the material, and also to the process of obtaining the composite [70–73]. The longer the VR fibres, the greater the number of voids present in the composite, resulting in poor dispersion of the fibres in the

Table 2: Comparison of results.

Fibre	Fibre volume fraction (%)	Matrix	Tensile stress (MPa)	Young's modulus (GPa)	Flexural stress (MPa)	Flexural modulus (GPa)	Absorption rate (%)	Use	Ref
Cotton fibres from textile waste	0.1; 0.2; 0.3; 0.4	Epoxy	49.5–75.4	1.5–3.3	46.4–108.4	2.6–7.1	4.6–8.3	a	[83]
Pineapple fibre from the leaves	10; 20; 30; 40	Polyester	7–29	0.51–0.76	18–31	0.39–0.7	0.2–0.3	a; b	[80]
Flax fibre	—	Epoxy	—	18.6–20.4	—	—	25.7	a	[102]
Bauhinia racemosa fibre	10; 20; 30; 40; 50	Polyester	4.8–18.8	—	9.8–34.1	—	2.2–4.1	a; b; c	[81]
Banana fibre from the pseudo stem	20; 40; 60	Epoxy	—	—	—	—	9.7–83.1	a; b	[79]
Empty oil palm fruit fibre	10; 20; 30; 40; 50; 60; 70	Polyester	0.1–3.9	0.002–0.023	—	—	3.1–9.0	a	[82]
Oil palm mesocarp fibre	0; 2.5; 5; 7.5; 10; 12.5; 15	Polyester	8.3–11.3	2.930–3.318	22.36–61.7	1.218–2.319	0.131–17.064	b	[41]
Raphia vinifera fibre	0; 20; 30; 40	Epoxy	05.68–13.64	1.332–1.912	14.68–26.77	1.528–2.596	36.12–71	a; b	Present work

a: automotive components; b: building industry; c: sports equipment.

matrix, thus creating a settling phenomenon. This observation has also been reported by Habibi et al. [74] on a nonwoven linen-reinforced composite and by Tiaya et al. [75] on a hybrid composite with RV and *Bambusa vulgaris* particles.

Figure 2(d) shows the evolution of the absorption rate as a function of the fibre volume fraction in the composite. It is observed that increasing the fibre length from 5 to 15 mm increases the water absorption rate in the composite compared to the 0% fibre formulation. This increase in the rate of water absorption in the composite as the length of the *Raphia Vinifera* Fibre (RVF) increases is due to the fact that the inclusion of long fibres decreases the stacking density of the composite, resulting in poor fibre distribution and the presence of the porosity shown in Figure 2(c). This presence of raffia fibre clusters in the matrix can act as a water reservoir due to the hydrophilic nature of lignocellulosic fibres [76, 77]. These observations have also been reported by Das and Biswas [78] on the characterisation of epoxy matrix composites reinforced with coir fibres. Similarly, increasing the fibre volume fraction to 40% also increases the water absorption rate compared to the 20% fibre formulation. This evolution of the water absorption rate is consistent with the evolution of the porosity presented in Figure 2(c), according to which the evolution of the porosity of the composite gives information on the capacity of the composite to absorb water [41]. Thus, the formulation EP-RVF 20-5 has the lowest absorption rate (36.12%), while the formulation EP-RVF 40-15 has the highest absorption rate (71%) compared to EP-RVF 0. The absorption rate of EP-RVF is comparable to the literature on plant fibre-reinforced composites presented in Table 2 [41, 79–83] and could be explained by the fact that RVF is very hydrophilic with an absorption rate between 303% and 662% [21]. This suggests that treatment to reduce the high hydrophilicity of RVF should be considered before introducing it as a composite reinforcement, as suggested by Huisken et al. [41].

3.2. Mechanical Characterisation of EP-RVF

3.2.1. Mechanical Properties in Tensile Tests. An extract of the tensile curves for the different formulations (0%, 20%, 30%, and 40%) and lengths (5, 10 and 15 mm) of the EP-RVF composites are presented in Figure 3(a), and the tensile fractured sample of the EP-RVF 30-5 formulation is presented in Figure 3(b). The observation of the stress–strain curve shows that the composite fails abruptly when the load becomes maximum, which is characteristic of brittle behaviour and could be attributed to the brittle nature of RVF [37]. Similar behaviour is reported by Gonçalves et al. [26] on the development and characterisation of a RVF-reinforced composite from polyester matrix sheet, as well as the work carried out by Chin et al. [6] and Hassan et al. [48] on epoxy matrix composites with bamboo and *B. vulgaris* fibre reinforcements, respectively.

Figures 4(a) and 4(b) show the Young's modulus and tensile strength results of the EP-RVF composite. It can be seen that the mechanical properties of the composite are lower than that of the matrix. Such behaviour was observed by Filho et al., [26] on RVF-reinforced composites from the sheet. Compared to the 0% fibre formulation, the tensile Young's modulus of the composites decreases from 9.98% to 30.33% for the 20% fibre volume fraction, from 9.99% to 16.98% for the 30% fibre composites, from 13.11% to 28.44% for 40% fibre composites, and the stress decreases by a value between 26.72% and 58.48% for the 20% fibre volume fraction, between 20.74% and 47.73% for the 30% fibre volume fraction, between 22.23% and 55.05% for the 40% fibre volume fraction. Thus, increasing the fibre volume fraction increases the Young's modulus and stress

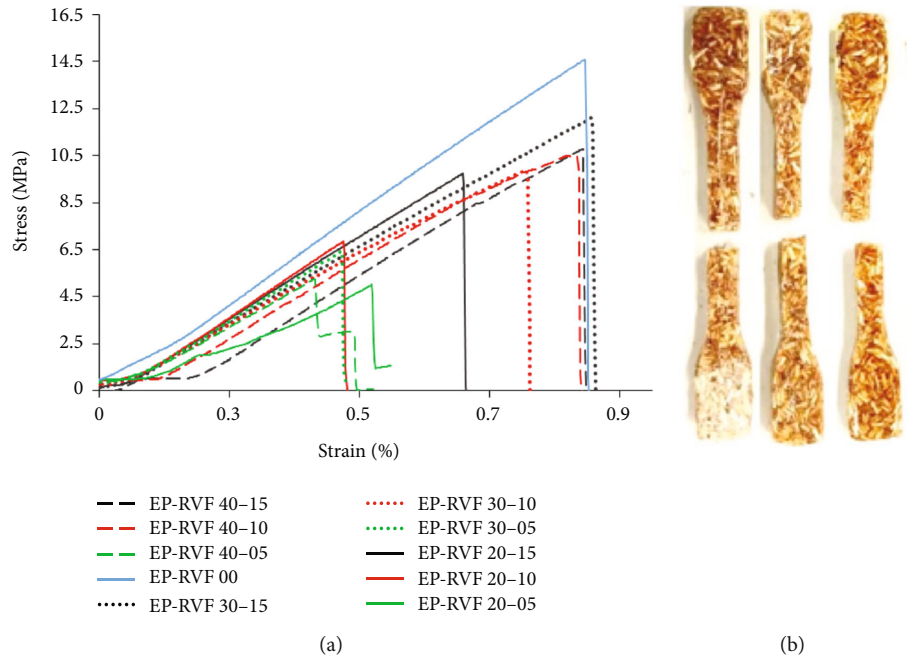


Figure 3: Typical (a) tensile stress–strain curve and (b) broken specimens in the tensile test of EP-RVF 30-5.

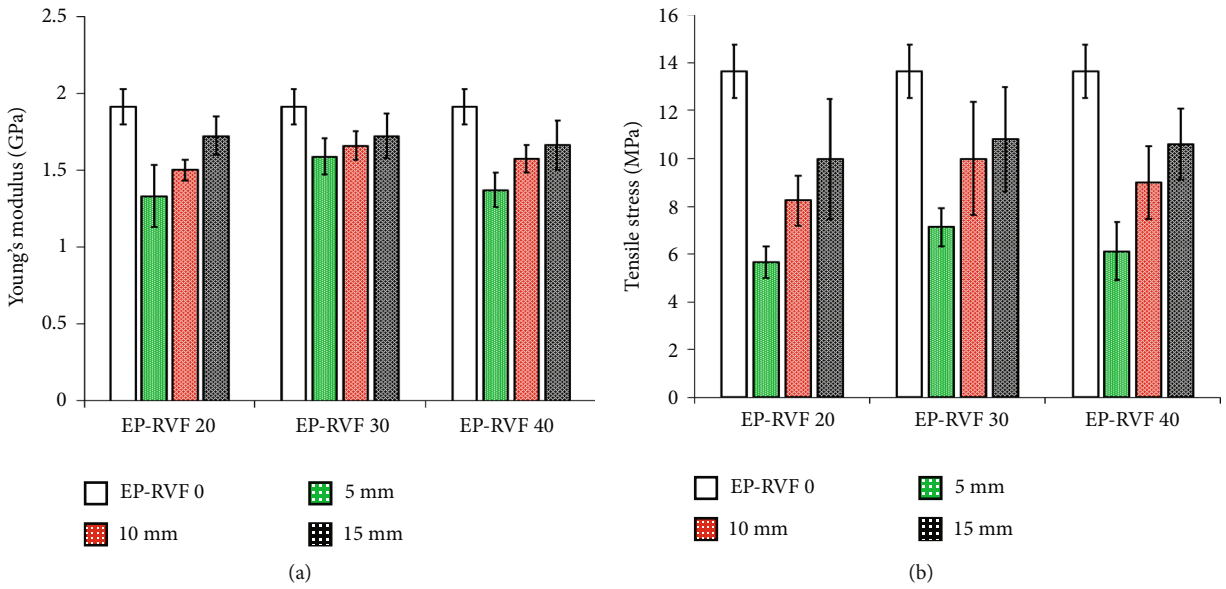


Figure 4: Mechanical properties in tensile test: (a) Young's modulus and (b) strength.

up to a threshold of 30% after which these characteristics decrease. This behaviour has been observed in previous works [10, 83] and could be attributed to the interfacial bond between the fibre and the matrix [84]. At a fibre volume fraction of 20%, the fibres have a low capacity to transfer loads to each other resulting in poor tensile mechanical properties [85]. However, at 30% fibre volume fraction, the fibres participate better in stress transfer [86], whereas a high fibre volume fraction of 40% leads to a poor distribution of fibres in the composite, creating agglomerations that block the stress transfer, thus leading to this decrease [76, 86, 87].

Figures 4(a) and 4(b) reveal that the tensile stress and Young's modulus increase with fibre lengths while remaining lower than those of the matrix alone. Thus, the tensile stress increases from 5.66 to 9.47 MPa for the 20% fibre composite, while the Young's modulus increases from 1.32 to 1.71 GPa for the same fibre volume fraction for respective fibre lengths from 5 to 15 mm. This trend in mechanical properties as a function of lengths is also observed for the 30% and 40% fibre formulations. For example, the Young's modulus of the 30% fibre formulation increases by 4.24% and 8.13% for the 10 and 15 mm fibre lengths, respectively, compared to the 5 mm fibre composite. For the 40% fibre

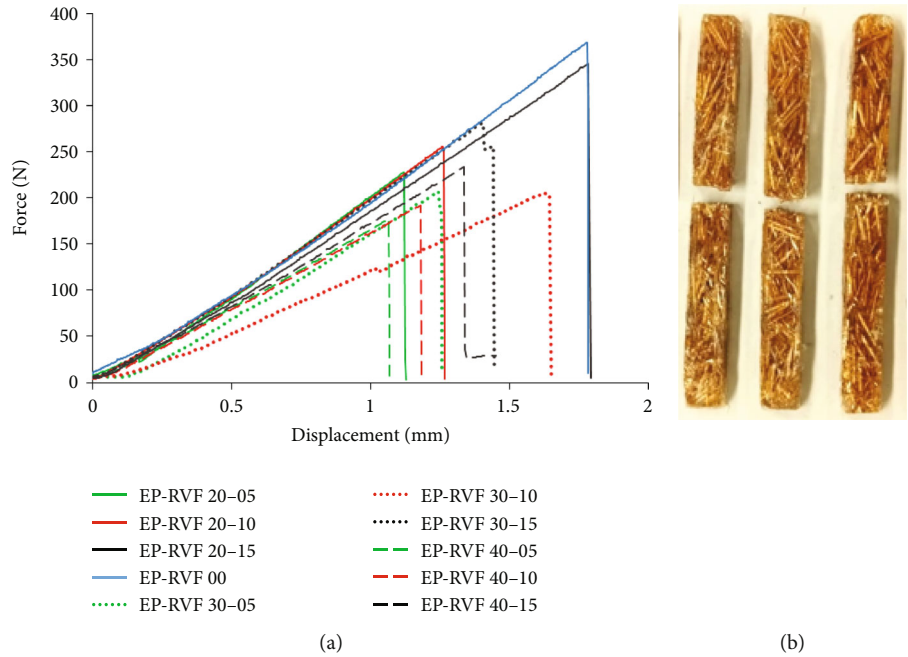


Figure 5: Typical (a) three-point bending displacement force curve and (b) broken specimens in the bending test of EP-RVF 30-15.

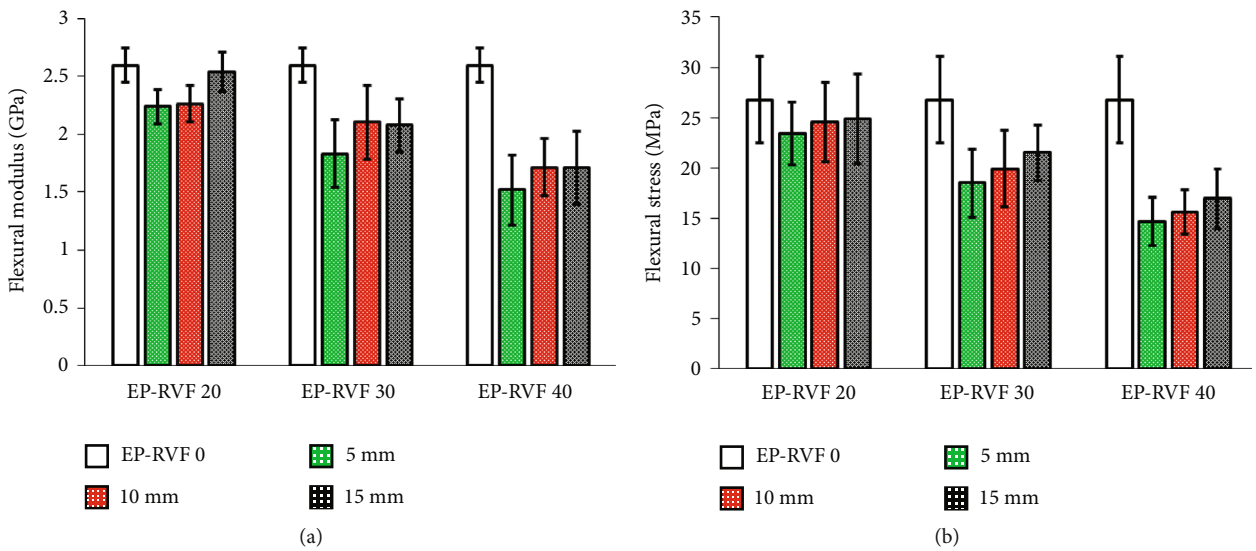


Figure 6: Flexural mechanical properties of EP-RVF: (a) stress and (b) flexural modulus.

formulation, the modulus increases by 12.97% and 17.63% for the 10 and 15 mm lengths, respectively, compared to the 5 mm lengths. The tensile stress of the 30% and 40% fibre composites increases by 9.62%–34.04% and 31.81%–42.16%, respectively, compared to the same volume fraction and 5 mm fibre lengths composites. This trend of increasing characteristics with increasing fibre lengths in the composite has been observed in other works [88, 89] and could be attributed to the critical length (l_c) of the fibre [90] determined through Equation (22). This study is carried out with fibres of length between 2lc and 5lc. In terms of the influence of these fibre lengths on the said mechanical properties, there is a correlation between the critical length, the stress, and the Young's modulus in tension, which is explained by the fact that as the critical length increases, the mechanical properties also increase. Such a phenomenon is also highlighted by Joseph et al. [88] and confirmed by Sathishkumar et al. [89] who showed that the tensile stress and modulus increase up to a threshold of 10lc.

3.2.2. Mechanical Properties in Three-Point Bending. An extract of the bending curves for the different formulations (0%, 20%, 30%, and 40%) and fibre lengths (5, 10, and 15 mm) of the EP-RVF composites are presented in Figure 5(a), and the specimens fractured after a three-point bending load of the EP-RVF 30-15 formulation are presented

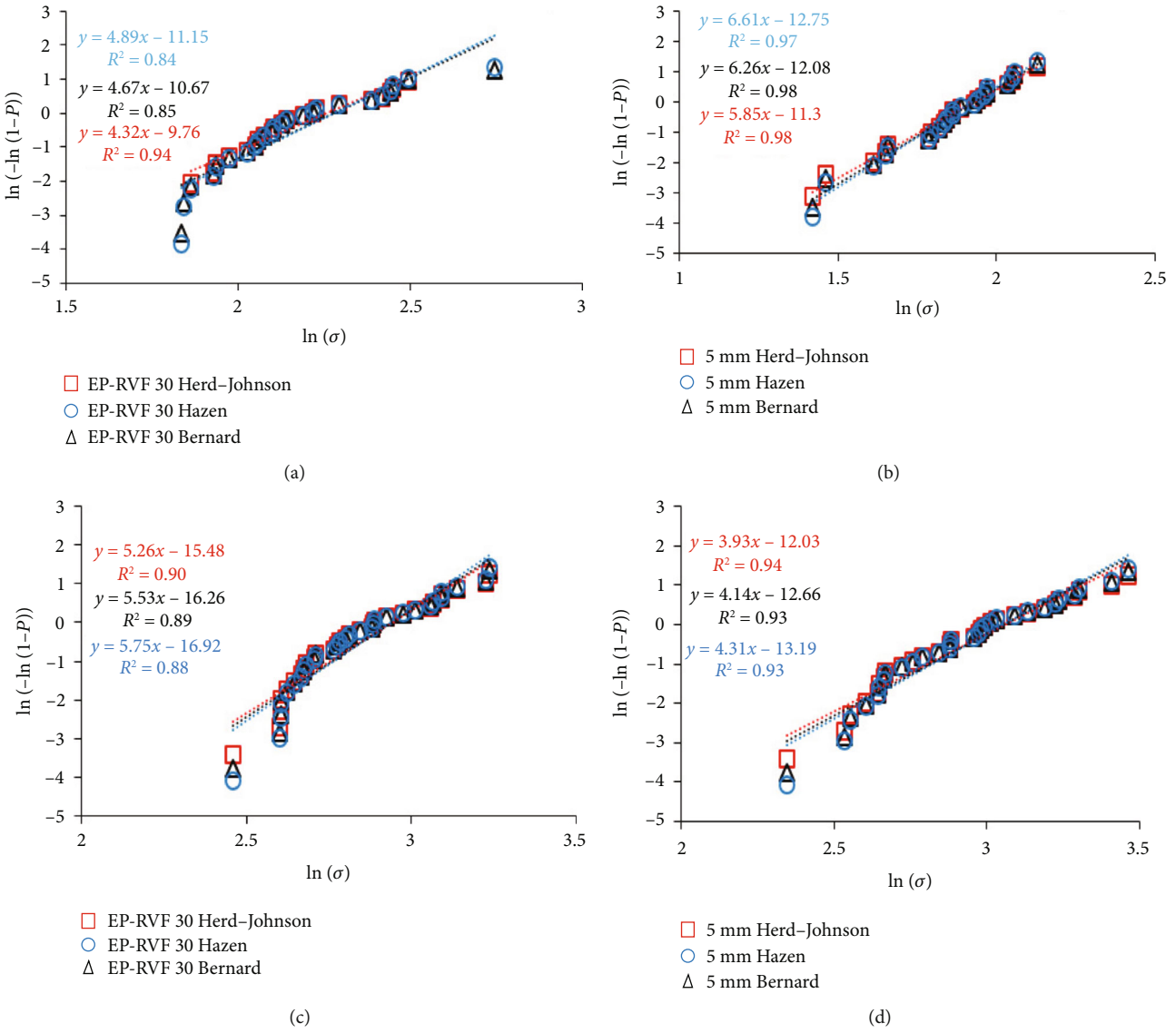


Figure 7: Determination of Weibull parameters: (a) tensile for fibre rate, (b) tensile for lengths, (c) bending for fibre rate, and (d) bending for lengths.

in Figure 5(b). In general, a sudden failure of the specimens is observed as soon as the force reaches the maximum characteristic of brittle materials, which is in line with the work of other researchers on the characterisation of flax and hemp plant fibre composites [91] and piassava [9].

The evolution of the three-point bending strength and flexural modulus of EP-RVF composites as a function of fibre volume fraction and lengths are presented in Figures 6(a) and 6(b), respectively. The general observation shows that the *RVF* lower the three-point bending mechanical characteristics of the composites compared to the matrix alone. It is also observed that the stress and flexural modulus decrease with increasing fibre volume fraction in the composite with greater properties attributed to the 20% fibre formulation compared to the 40% formulation. Thus, the flexural strength of composites containing 5, 10, and 15 mm fibres at 20% fibre volume fraction are 23.41, 24.55, and 24.82 MPa, respectively, while their flexural modulus values are 2.23, 2.26, and 2.53 GPa, respectively. The bending stress evolves with a tendency that increasing the fibre volume fraction slightly decreases the mechanical properties. This trend is opposite to that generally observed by other authors working on composites reinforced with fibres of plant origin, which rather shows that increasing the fibre volume fraction up to a threshold increases the mechanical properties [71, 90, 92, 93]. This can be attributed to the high porosity of the composites as presented in Figure 2(c) compared to the 0% fibre composite. Similarly, Huisken et al. [41] reveal that the high porosity rate leads to a decrease in the mechanical characteristics of the composite. According to the authors, this is linked to the poor distribution of fibres in the matrix [94], resulting in a low wettability of the fibres during the polymerisation process in the matrix for the 30% and 40% fibre volume fractions [95, 96].

Compared to the 0% fibre formulation, the flexural modulus of the composites decreases from 2.23% to 13.76% for the 20% fibre volume fraction, from 29.58%

Table 3: Weibull parameters in tensile.

		Lengths			Volume fraction		
		5 mm	10 mm	15 mm	20%	30%	40%
Average tensile strength	σ_m	6.41	9.22	10.29	9.02	8.94	8.49
	m	5.85	5.08	4.95	3.44	4.32	3.53
Herd–Johnson	σ_0	6.90	10.01	11.22	10.04	9.55	9.44
	R^2	0.98	0.95	0.95	0.96	0.94	0.98
	m	6.26	5.43	5.27	3.65	4.68	3.75
Bernard	σ_0	6.88	9.98	11.18	10.01	9.78	9.41
	R^2	0.98	0.91	0.96	0.95	0.85	0.97
	m	6.61	5.73	5.54	3.84	4.89	3.94
Hazen	σ_0	6.87	9.96	11.15	9.98	9.76	9.38
	R^2	0.97	0.89	0.95	0.94	0.84	0.97
Added value of Anderson Darling	p	0.67	0.18	0.80	0.39	0.07	0.54

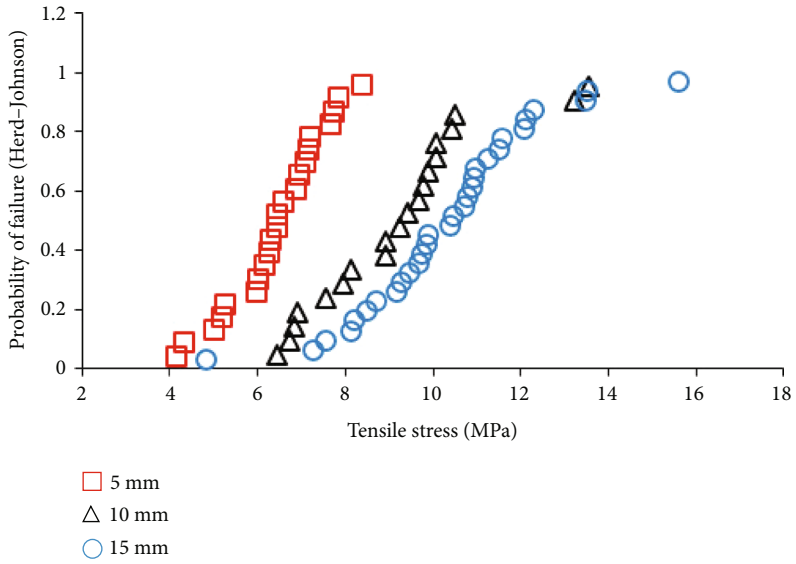
Table 4: Weibull parameters in three-point bending.

		Lengths			Volume fraction		
		5 mm	10 mm	15 mm	20%	30%	40%
Average bending strength	σ_m	19.33	19.55	21.07	24.26	17.47	18.21
	m	3.93	4.07	4.08	4.7	5.26	4.81
Herd–Johnson	σ_0	21.33	21.46	23.22	26.48	18.95	19.85
	R^2	0.94	0.92	0.90	0.97	0.90	0.96
	m	4.14	4.55	4.28	4.95	5.53	5.07
Bernard	σ_0	21.27	21.41	23.17	26.42	18.92	19.81
	R^2	0.93	0.90	0.89	0.96	0.89	0.95
	m	4.31	4.73	4.45	5.17	5.75	5.29
Hazen	σ_0	21.22	21.37	23.13	26.37	18.89	19.77
	R^2	0.93	0.89	0.88	0.96	0.88	0.94
Added value of Anderson Darling	p	0.67	0.19	0.81	0.39	0.07	0.54

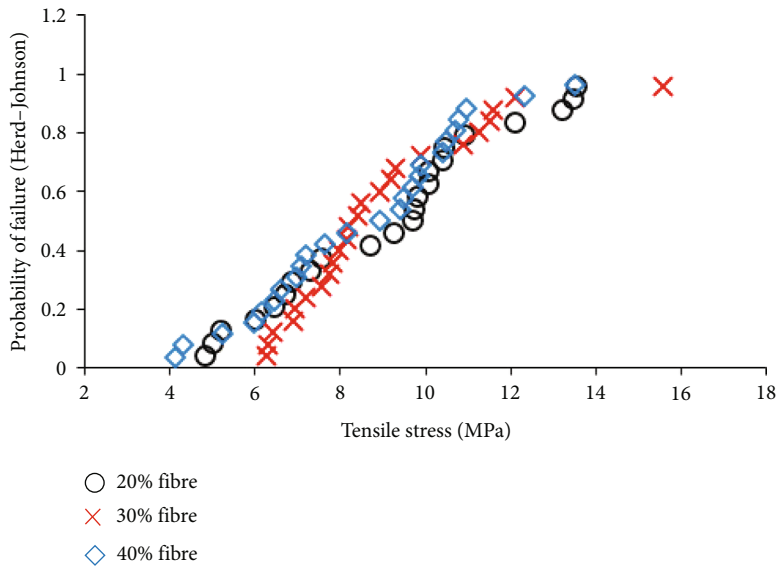
to 20.01% for the 30% fibre composites, from 34.02% to 41.51% for 40% fibre composites, and the stress decreases between 7.27% and 12.55% for the 20% fibre volume fraction, between 19.7% and 30.99% for the 30% fibre volume fraction, between 36.87% and 45.17% for the 40% fibre volume fraction.

Growth in flexural modulus and bending stress is observed with increasing fibre lengths of 5, 10, and 15 mm in the composite, although these values remain lower than those of the unreinforced composite. Introducing the 15 mm fibre length at 20%, 30%, and 40% into the matrix provides high flexural modulus values of 1.71, 2.03, and 2.53 GPa, respectively, compared to 5 and 10 mm. Similarly, the highest values of bending stress for the 20%, 30%, and 40% fibre composites (16.9, 21.5, and 24.82 MPa, respectively) were observed for the 15 mm lengths. These results may be due to the fact that longer fibres are capable of better anchorage, which resists bending loads by improving stress and flexural modulus [88, 89]. In addition, the length of the fibres effectively participated in improving the load transfer in the composite, hence the improved properties through increasing the fibre lengths.

3.3. Weibull Statistical Analysis. Figures 7(a)–7(d) show an extract of the linearisation curves in tensile and three-point bending and the parameters of the two-factor Weibull analysis for the different approaches to determine the probability (Herd–Johnson, Bernard, and Hazen) of failure of composites. With the lengths and fibre volume fraction of the composites taken into account, the summary of the Weibull parameters after the tensile test contained in Table 3 and the three-point bending test presented in Table 4 show that the composite fracture follows a Weibull distribution and the Herd–Johnson approximation of the probability of fracture correlates better with the experimental results of both the tensile test properties and the three-point bending test properties. Similar results have also been reported in the literature by Issasfa et al. [64] on plant fibre composites, which show that the Herd–Johnson probability of failure better approximates the experimental results. In tensile, the Weibull modulus decreases with increasing fibre lengths (5, 10, and 15 mm), reflecting an increase in the strength of the composite, as presented in Table 3. This observation is in agreement with the results of Ray et al., [97]. However, increasing the fibre volume fraction between 20% and 30%



(a)



(b)

Figure 8: Continued.

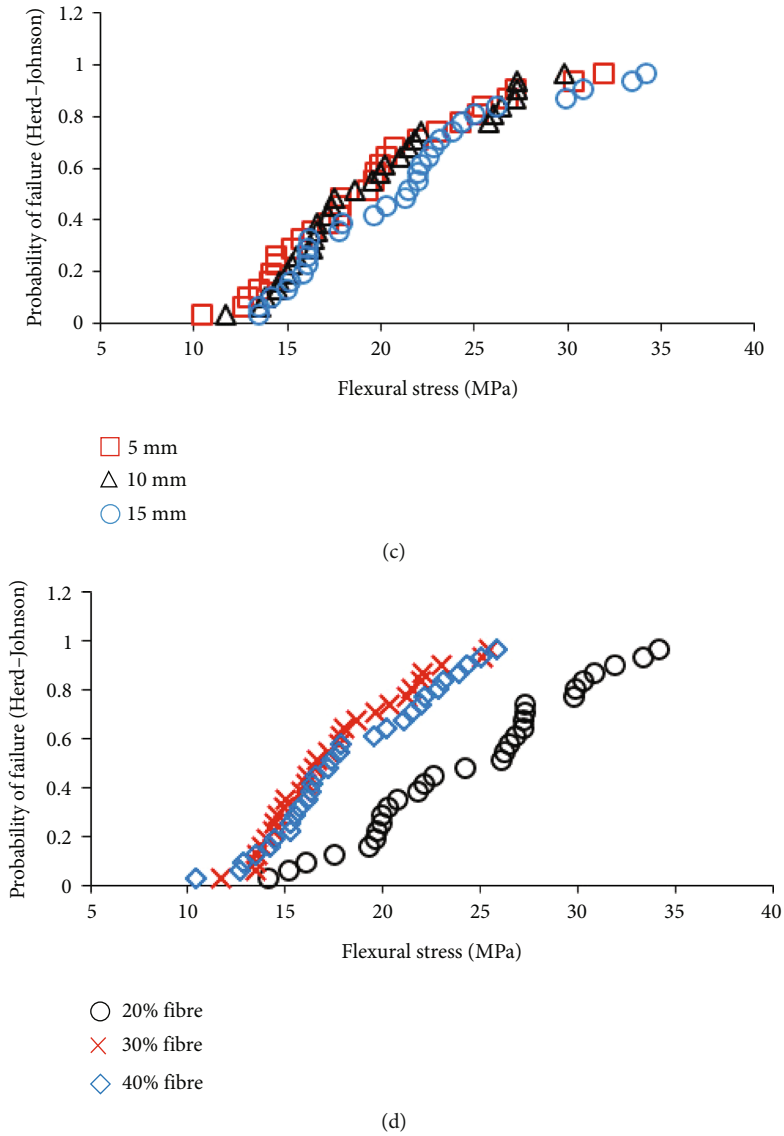


Figure 8: Herd–Johnson failure probability: (a) bending and fibre lengths, (b) bending and fibre rate, (c) tensile and fibre lengths, and (d) tensile fibre rate.

increases the Weibull modulus [61], and increasing the fibre volume fraction between 30% and 40% lowers the Weibull modulus. In three-point bending, the Weibull modulus increases with a length increase between 5 and 15 mm, reflecting an increase in strength (Table 4), characteristic of the brittle behaviour of the composite contrary to the observations of Quintero-Davila et al. [98] who observed a decrease in Weibull modulus attributed to the ductility of the fibre incorporated in a cementitious matrix. It is also observed that the Weibull modulus and flexural strength evolve similarly for the fibre volume fraction of EP-RVF, reflecting a wide dispersion of flexural strength, as observed by Trujillo et al. [99].

The Weibull modulus is very low ($m < 20$) in Tables 3 and 4 for all combinations of fibre lengths (5, 10, and 15 mm) and volume fraction (20%, 30%, and 40%), reflecting the fact that the brittle fracture of the composite is only due to the tensile and three-point bending test loading of the composite, as expressed by Sayeed et al. [100].

Figures 8(a)–8(d) show the Herd–Johnson fracture probability curves for the three-point bending test and the tensile test as a function of fibre lengths (5, 10, and 15 mm) and fibre volume fraction (20%, 30%, and 40%) in the composite. As previously mentioned, it can be seen that increasing the fibre lengths between 5 and 15 mm (Figure 8(a)) leads to higher tensile strength, while the reinforcement volume fraction (Figure 8(b)) between 20% and 30% slightly increases tensile strength [98] and decreases between 30% and 40%. After the three-point bending test, increasing the lengths (Figure 8(c)) between 5 and 15 mm slightly increased the mechanical properties, while increasing the fibre volume fraction (Figure 8(d)) lowered the mechanical properties of the composite earlier.

3.4. MANOVA of Mechanical Properties. Table 5 shows the parameters of the multivariate test of variance of the three-point bending properties of the EP-RVF composite. It is

Table 5: MANOVA in bending.

Effect		Value	D	ddl of the hypothesis	Error ddl	Sig.	Partial squared eta
Volume fraction	Pillai's trace	1.268	2.887	6	10	0.067	0.634
	Wilks' Lambda	0.124	2.459	6	8	0.09	0.648
	Hotelling trace	3.921	1.960	6	6	0.017	0.662
Lengths	Pillai's trace	0.213	0.198	6	10	0.070	0.106
	Wilks' Lambda	0.793	0.164	6	8	0.080	0.110

D: sum of squares; ddl: degree of freedom; sig.: plus-value or Fischer probability.

Table 6: Tukey bending test for fibre volume fraction and lengths.

Dependent variable	Variables (volume fraction and lengths)		Difference in means (I–J)	Standard error	Sig.	90% confidence interval	
	(I)	(J)				Lower terminal	Upper limit
Flexural modulus	0%	20%	332.8	165.7	0.282	143.5	809.2
		30%	754.4*	165.7	0.015	278.0	1230.7
		40%	771.3*	165.7	0.014	294.9	1247.7
Bending stress	0%	20%	−0.669	2.445	0.992	−7.699	6.35
		30%	6.117	2.445	0.157	−1.912	13.14
		40%	5.377	2.445	0.226	−1.652	12.40
Flexural modulus	0 mm	5 mm	643.1*	165.7	0.031	166.7	1119.4
		10 mm	653.1*	165.7	0.029	176.7	1129.5
		15 mm	562.3*	165.7	0.054	85.9	1038.7
Bending stress	0 mm	5 mm	4.261	2.445	0.381	−2.985	11.29
		10 mm	4.044	2.445	0.420	−0.912	11.07
		15 mm	2.519	2.445	0.740	−4.510	9.54

*Significant difference.

Table 7: Tensile MANOVA.

Effect		Value	D	ddl of the hypothesis	Error ddl	Sig.	Partial squared eta
Volume fraction	Pillai's trace	1.017	1.723	6	10	0.213	0.508
	Wilks' Lambda	0.13	2.368	6	8	0.129	0.640
Lengths	Pillai's trace	1.066	1.901	6	10	0.176	0.533
	Wilks' Lambda	0.03	6.428	6	8	0.010	0.828

D sum of squares, ddl: degree of freedom, sig.: plus-value or Fischer probability.

observed that the plus-value is less than 0.1 (90% confidence level), so the hypothesis of the significant impact of lengths and volume fraction on the mechanical bending properties of the composites is validated. Table 6 shows the Tukey test for lengths and fibre volume fraction of the EP-RVF composite. It can be seen that at the 90% confidence level, the flexural modulus drops significantly for fibre volume fractions of 30% and 40% with the greatest impact obtained at 40% of fibre compared to the 0% fibre formulation. The flexural modulus is significantly impacted by all fibre lengths in the composite compared to the 0% fibre formulation, with the 5 mm lengths having the greatest influence on flexural modulus. The bending stress is not significantly affected by the lengths of the fibres in the composite. On the other hand, the stress is not significantly influenced by the volume fractions and lengths compared to the 0% fibre formulation in the composite.

Table 7 shows MANOVA of the tensile mechanical properties of the EP-RVF composite. It is observed that the fibre volume fraction and lengths have a significant impact on the mechanical tensile behaviour of the composites, as the plus-value is above the confidence level. Table 8 shows the Tukey test for fibre volume fraction and lengths of the EP-RVF composite. It is observed that the fibre volume fractions significantly lowered the Young's modulus compared to the 0% composite with the greatest impact at 40% of fibre volume fraction. Similarly, tensile stress shows the greatest impact at 30% of fibre volume fraction compared to the 0% composite. In addition, all fibre lengths significantly lowered the Young's modulus and stress compared to the 0%

Table 8: Tukey tensile test for fibre volume fraction and lengths.

Dependent variable	Variables (volume fraction and lengths)		Difference in means (*I*–*J*)	Standard error	Sig.	90% confidence interval	
	(*I*)	(*J*)				Borne inférieure	Limite supérieure
Flexural modulus	0%	20%	439.4*	87.3	0.009	188.4	690.4
		30%	407.0*	87.3	0.014	156.0	658.0
		40%	475.7*	87.3	0.006	224.7	726.7
Bending stress	0%	20%	6.781*	0.918	0.001	4.142	9.420
		30%	6.606*	0.918	0.001	3.967	9.245
		40%	6.754*	0.918	0.001	4.115	9.392
Flexural modulus	0 mm	5 mm	580.6*	87.3	0.002	329.6	831.5
		10 mm	433.0*	87.3	0.010	182.0	684.0
		15 mm	308.6*	87.3	0.046	57.64	559.6
Bending stress	0 mm	5 mm	9.025*	0.918	0.000	6.386	11.66
		10 mm	6.255*	0.918	0.002	3.616	8.89
		15 mm	4.861*	2.445	0.007	2.222	7.50

*: significant difference.

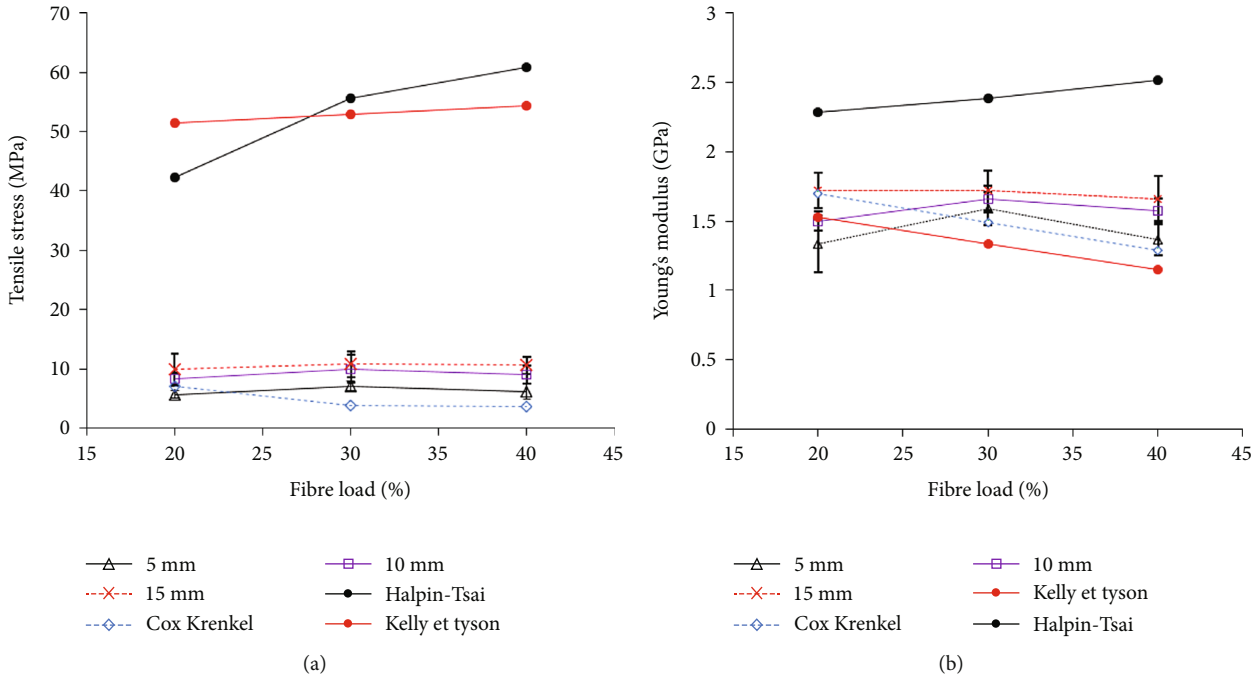


Figure 9: Mathematical homogenisation in tensile (a) stress and (b) Young's modulus.

composite, with the 5 mm long fibres having the greatest significant impact on both Young's modulus and tensile stress.

3.5. Mathematical Homogenisation. Figure 9(a) shows the evolution of the theoretical and experimental tensile strength models. It can be seen that the Cox–Krenkel model provides a better approximation of the experimental results with a relative error between the EP-RVF 20-5 samples estimated at 20.41%, for the EP-RVF 30-5 with a relative error of 18% and for the EP-RVF 40-5 an estimated error of 18.89%, while the theoretical models of modified HT and that of Kelly and Tyson are far from the experimental results so the relative error is respectively between [52.08–89.9]% and [75.41–89.01]%. It should be noted that the works on the prediction of the mechanical characteristics of plant fibre-reinforced composites mainly present the mathematical modelling of the Young's modulus to the detriment of the mechanical tensile strength [15, 67, 68, 101]. This could be explained by the large discrepancy between the experimental strength results obtained and the theoretical results that were obtained and presented in Figure 9(a) for the modified HT model and Kelly and Tyson, respectively.

Figure 9(b) shows the evolution of the theoretical and experimental results of Young's modulus. A better correlation between the Cox–Krenkel theoretical model and the experimental results of the EP-RVF 20 samples of 10–15 with a relative error between 1.34% and 15.77% is observed, while the Kelly and Tyson model better approximates the experimental results of the EP-RVF 30-5 samples with an error of 6.41% and EP-RVF 40-05 with an error of 6.15%, which is in congruence with the studies on the plant fibre-reinforced composite [15]. However, regardless of the formulation, the modified HT model shows the worst approximation of Young's modulus compared to the experimental results for samples EP-RVF 20-10, EP-RVF 20-15, EP-RVF 30-10 and 15 and EP-RVF 40-10 and 15 mm with deviations between the theoretical and experimental Young's modulus in the ranges [24.04–41.60%]%, [23.47–33.47%]%, and [24.46–5.54]%, respectively. Such behaviour was also observed on the plant fibre-reinforced composite [15] in contrast to the studies of Huisken et al. [41] for which the modified HT model correlates well with the experimental results.

It should be recalled that the main factor explaining the difference between the analytical results using the modified HT, Cox–Krenkel, and Tyson and Kelly methods and the experimental results is that the HT model assumes a perfect bond between the phases of the composite.

4. Conclusion

The present work was devoted to characterise the RV short random fibre composite material from a mechanical and physical point of view. Experimental data on mechanical behaviour were subjected to Weibull analysis and to test the prediction of the mathematical models. The composite, produced by contact moulding, consisted of a combination of three lengths (5, 10, and 15 mm) and three volume fractions (20%, 30%, and 40%) of RVF with epoxy resin as matrix. The results of the various characterisations showed that in physical terms, the absorption rate and porosity rise with increasing fibre lengths and volume fraction in the range of 36%–71% for absorption rate and 41.1%–58.1% for porosity compared to the unreinforced composite. In addition, the 5 mm EP-RVF 20 sample shows the lowest porosity as well as water absorption rate. Although the apparent and real densities decreased with increasing fibre rate and lengths with the 15 mm EP-RVF 40 sample having the lowest densities. In terms of mechanical characterisation, reinforced composites have a brittle behaviour and confirmed by Weibull analysis. In addition, the RVF do not behave as reinforcements in the composite as they have decreased the mechanical properties in tensile and three-point bending compared to the EP-RVF 0 sample. However, the causes may be due to the impact of porosities in the fibre, poor fibre/matrix adhesion, and to remedy this, we can consider alkaline and silane surface treatments of the fibres to improve the performance of the composite. A MANOVA analysis showed that the 5 mm and 40% lengths had a greater impact on the flexural modulus, while a 30% volume fraction of the 15 mm fibres significantly lowered the Young's modulus, and the EP-RVF 30-15 formulation had the best properties after fibre insertion. However, the tensile properties showed that the 10 mm and 40% lengths had a greater impact on the tensile Young's modulus, while a 30% volume fraction of the 5 mm fibres significantly lowered the strength besides, the EP-RVF 20-15 formulation had the best properties. An analysis of the mechanical properties in tensile and three-point bending showed that the brittle failure of the composite could be predicted by the Weibull criterion and the Herd–Johnson approximation correlated better with the experimental results.

The mathematical models of modified HT, Cox–Krenkel, and Tyson and Kelly were used to predict the Young's modulus and tensile strength of the composite. It was found that the Cox–Krenkel model correlates best with the experimental results. In view of its mechanical and physical characteristics, the present material could be used as reinforcement parts for vehicle backrests or interior decoration in the construction industry. Given to its low density and these different characteristics, the present bio-composite would make structures lighter without being less efficient, thus promoting energy savings. The very high porosity rate, the low mechanical properties of the RVF-based composite compared to pure resin, the behaviour of the fibres in the matrix, and the analysis of the microstructure could be limitations of the present work. It would therefore be advisable to consider specific treatments on the fibres as well as a study of the behaviour of the composite at the microscopic scale.

Data Availability

The data used to support the findings of this study are available from the corresponding author upon request.

Conflicts of Interest

The authors declare that they have no conflicts of interest.

Authors' Contributions

Tchinwoussi Youbi Syrille Brice: conceptualisation, investigation, data retention, formal analysis, methodologies, data curation, software, writing-preparation of original draft, and editing. Harzallah Omar: conceptualisation, supervision, review, and validation. Sikame Tagne Nicodème Rodrigue: conceptualisation, methodology, supervision, review, and validation. Huisken Mejouyo Paul William: conceptualisation, methodology, supervision, review, and validation. Tido Tiwa Stanislas: conceptualisation, methodology, supervision, review, and validation. Drean Jean-Yves: supervision, review, and validation. Sophie Bistac-Brogly: conceptualisation, methodology, supervision, review, and validation. Njeugna Ebenezer: conceptualisation, supervision, review, and validation.

Acknowledgments

The authors would like to thank the Laboratoire de Physique et Mécanique Textile (LPMT), ENSISA—Université de Haute Alsace, France, for hosting and facilitating the mechanical tests on the various samples.

References

[1] B. Y. Kai Zhang, F. Wang, W. Liang, Z. Wang, and Z. Duan, "Thermal and mechanical properties of bamboo fiber reinforced epoxy composites," *Polymers*, vol. 10, pp. 1–18, 2018.

[2] J. Huang and W. Young, "The mechanical, hygral, and interfacial strength of continuous bamboo fiber reinforced epoxy composites," *Composites Part B: Engineering*, vol. 18, pp. 1–29, 2019.

[3] A. Gupta, "Synthesis, chemical resistance, and water absorption of bamboo fiber reinforced epoxy composites," *Polymer Composites*, vol. 37, pp. 141–145, 2014, 2020.

[4] M. Martina and D. W. Hutmacher, "Biodegradable polymers applied in tissue engineering research: a review," *Polymer International*, vol. 157, pp. 145–157, 2005, 2007.

[5] R. Jeyapragash, V. Srinivasan, and S. Sathiyamurthy, "Mechanical properties of natural fiber/particulate reinforced epoxy composites—a review of the literature," *Materials Today: Proceedings*, vol. 22, pp. 1–5, 2019.

[6] J. Chin, S. C. Tee, K. F. Tong, F. S. Ong, and H. R. Gimbun, "Thermal and mechanical properties of bamboo fiber reinforced composites," *Materials Today Communications*, vol. 23, pp. 1–14, 2020.

[7] M. R. Sanjay, G. R. Arpitha, L. L. Naik, K. Gopalakrishna, and B. Yogesha, "Applications of natural fibers and its composites: an overview," *Natural Resources*, vol. 7, no. 3, pp. 108–114, 2016.

[8] L. Kerni, S. Singh, A. Patnaik, and N. Kumar, "A review on natural fiber reinforced composites," *Materials Today: Proceedings*, vol. 28, pp. 1616–1621, 2020.

[9] R. G. Castro, F. C. Amorim, and J. Reis, "Effects of fiber length on the performance of piassava-reinforced epoxy composites," *Journal of Materials: Design and Applications*, vol. 234, pp. 1–8, 2020.

[10] M. Kamble, P. S. Sampath, and S. Sagadevan, "Influence of fiber length, fiber content and alkali treatment on mechanical properties of natural fiber-reinforced epoxy composites," *Polimery/Polymers*, vol. 64, no. 2, pp. 93–99, 2019.

[11] N. Syafiqaz, N. Arman, R. S. Chen, and S. Ahmad, "Review of state of the art studies on the water absorption capacity of agricultural fiber reinforced polymer composites for sustainable construction," *Construction and Building Materials*, vol. 302, pp. 1–14, 2021.

[12] S. Bhaskara, R. Devireddy, and S. Biswas, "Thermo-physical properties of short banana – jute fiber-reinforced epoxy-based hybrid composites," *Journal of Materials: Design and Applications*, vol. 232, pp. 1–13, 2016.

[13] F. Vilaseca, R. Del, R. Serrat, J. Alba, P. Mutje, and F. X. Espinach, "Macro and micro-mechanics behavior of stifness in alkaline treated hemp core fibres polypropylene-based composites," *Composites Part B: Engineering*, vol. 144, pp. 118–125, 2018.

[14] E. Osoka, "A modified Halpin–Tsai model for estimating the modulus of natural fiber reinforced composites," *International Journal of Engineering Science Invent*, vol. 7, no. 5, pp. 63–70, 2018.

[15] M. S. Pernevan and L. Marsavina, "The influence of the théorical fibers arrangement model on the mechanical properties of the vegetal fiber reinforced composites," *European Conference on Composite Materials*, vol. 15, pp. 24–28, 2012.

[16] S. Migneault, A. Koubaa, F. Erchiqui, A. Chaala, K. Englund, and M. P. Wolcott, "Application of micromechanical models to tensile properties of wood–plastic composites," *Wood Science and Technology*, vol. 45, pp. 1–12, 2010.

[17] A. K. Djoumessi, R. Nicodème, S. Tagne, T. T. Stanislas, F. Ngapgue, and E. Njeugna, "Optimization of the Young's modulus of woven composite material made by Raphia vinifiera fiber/epoxy," *International Journal for Simulation and Multidisciplinary Design Optimization*, vol. 21, p. 13, 2022.

[18] Y. Xu, L. Cheng, L. Zhang, D. Yan, and C. You, "Optimization of sample number for Weibull function of brittle materials strength," *Ceramics International*, vol. 27, pp. 239–241, 2001.

[19] J. Tanks, K. Naito, and H. Ueda, "Characterization of the static, creep, and fatigue tensile behavior of basalt fiber/polypropylene composite rods for passive concrete reinforcement," *Polymers*, vol. 13, no. 18, pp. 21–27, 2021.

[20] T. T. Stanislas, J. F. Tendo, E. B. Ojo et al., "Production and characterization of pulp and nanofibrillated cellulose from selected tropical plants," *Journal of Natural Fibers*, vol. 19, pp. 1–17, 2020.

[21] N. R. S. Tagne, E. Njeugna, M. Fogue, J. Drean, A. Nzeukou, and D. Fokwa, "Study of water absorption in Raffia vinifera fibres from Bandjoun, Cameroon," vol. 2014, pp. 1–11, 2014, *Hindawi Publishing Corporation*.

[22] T. N. E. Flore, Z. N. François, and T. M. Félicité, "Immune system stimulation in rats by Lactobacillus sp. isolates from Raffia wine (Raphia vinifera)," *Cellular Immunology*, vol. 260, no. 2, pp. 63–65, 2010.

[23] N. R. S. Tagne, N. Ebénézer, N. Dieunedort et al., "Investigation of the physical and mechanical properties of Raffia vinifera fibers along the stem," *Journal of Natural Fibers*, vol. 14, no. 5, pp. 621–633, 2017.

[24] E. Njeugna, N. R. S. Tagne, J. Drean, D. Fokwa, and O. Harzallah, "Mechanical characterization of Raffia fibres from 'raphia viniferaa'," *International Journal of Mechanical Structures*, vol. 3, no. 1, pp. 1–17, 2012.

[25] T. T. Stanislas, G. C. Komadja, Y. R. Nafu et al., "Potential of raffia nanofibrillated cellulose as a reinforcement in extruded earth-based materials," *Case Studies in Construction Materials*, vol. 16, pp. 1–11, 2022.

[26] E. G. d. O. Filho, F. S. da Luz, R. T. Fujiyama, A. C. R. da Silva, V. S. Candido, and S. N. Monteiro, "Effect of chemical treatment and length of raffia fiber (Raphia vinifera) on mechanical stiffening of polyester composites," *Polymers*, vol. 12, no. 12, pp. 1–17, 2020.

[27] M. F. Pucci, M. C. Seghini, and P. Liotier, "Surface characterisation and wetting properties of single basalt fibres," *Composites Part B: Engineering*, vol. 109, pp. 1–28, 2016.

[28] Q. Shen, D. Sen Liu, Y. Gao, and Y. Chen, "Surface properties of bamboo fiber and a comparison with cotton linter fibers," *Colloids Surfaces B Biointerfaces*, vol. 35, no. 3–4, pp. 193–195, 2004.

[29] H. Cai, "Wetting behavior and surface energy of bamboo fiber determined via dynamic contact angle analysis using the Wilhelmy technique," *BioResources*, vol. 14, no. 3, pp. 5121–5131, 2019.

[30] M. F. Pucci, P.-J. Liotier, D. Seveno, C. Fuentes, A. V. Vuure, and S. Drapier, "Wetting and swelling property modifications of elementary flax fibres and their effects on the liquid

composite moulding process," *Composites Part A: Applied Science and Manufacturing*, vol. 97, pp. 31–40, 2017.

[31] L. Q. N. Tran, C. A. Fuentes, C. Dupont-Gillain, A. W. Van Vuure, and I. Verpoest, "Wetting analysis and surface characterisation of coir fibres used as reinforcement for composites," *Colloids and Surfaces A: Physicochemical and Engineering Aspects*, vol. 377, no. 1–3, pp. 251–260, 2011.

[32] S. Khandelwal and K. Y. Rhee, "Recent advances in basalt-fiber-reinforced composites: tailoring the fiber–matrix interface," *Composites Part B: Engineering*, vol. 192, pp. 1–13, 2020.

[33] A. Benkhelladi, H. Laouici, and A. Bouchoucha, "Tensile and flexural properties of polymer composites reinforced by flax, jute and sisal fibres," *International Journal of Advanced Manufacturing Technology*, vol. 108, no. 3, pp. 895–916, 2020.

[34] C. Prakash, R. Vardhan, M. Faizul, A. Yadav, and V. Kumar, "Fabrication and evaluation of physical and mechanical properties of jute and coconut coir reinforced polymer matrix composite," *Materials Today: Proceedings*, vol. 38, pp. 2572–2577, 2021.

[35] Z. Kamble and B. K. Behera, "Mechanical properties and water absorption characteristics of composites reinforced with cotton fibres recovered from textile waste," *Journal of Engineered Fibers and Fabrics*, vol. 15, pp. 1–7, 2020.

[36] M. Jawaid and A. Khan, *Vegetable Fiber Composites and Their Technological Applications*, Springer Nature Singapore Pte Ltd, Singapore, 2021st edition, 2021.

[37] S. B. T. Youbi, N. R. Sikame Tagne, O. Harzallah et al., "Effect of alkali and silane treatments on the surface energy and mechanical performances of Raphia vinifera fibres," *Industrial Crops and Products Journal*, vol. 190, pp. 1–13, 2022.

[38] C. Baley, A. Le Duigou, A. Bourmaud, and P. Davies, "Influence of drying on the mechanical behaviour of flax fibres and their unidirectional composites," *Composites Part A: Applied Science and Manufacturing*, vol. 43, no. 8, pp. 1226–1233, 2012.

[39] F. X. Espinach, F. Julian, N. Verdaguer et al., "Analysis of tensile and flexural modulus in hemp strands/polypropylene composites," *Composites Part B: Engineering*, vol. 47, pp. 339–343, 2013.

[40] N. Defo, R. N. T. Sikame, W. P. M. Huisken et al., "Development and characterization of agglomerated abrasives based on agro-industrial by-products," *Journal of Natural Fibers*, vol. 20, no. 1, p. 18, 2023.

[41] P. W. M. Huisken, G. Tchemou, N. R. S. Tagne, D. Ndapeu, and E. Njeugna, "Effect of the addition of oil palm mesocarp fibers on the physical and mechanical properties of a polyester matrix composite," *International Journal of Polymer Science*, vol. 2022, p. 12, 2022.

[42] M. H. Dastmard, R. Ansari, and S. Rouhi, "Prediction of axial Young's modulus of epoxy matrix reinforced by group-IV nanotube: a finite element investigation," *Mechanics of Materials*, vol. 157, pp. 1–9, 2021.

[43] ASTM D792-07, "Standard test methods for density and specific gravity (relative density) of plastics," *American Society for Testing and Materials*, vol. 14, pp. 1–5, 2007.

[44] ASTM D2734-94, "Standard test methods for void content of reinforced plastics," *American Society for Testing and Materials*, pp. 1–3, 2003.

[45] ASTM D570-98, "Standard test method for water absorption of plastics," *American Society for Testing and Materials*, pp. 1–4, 1998.

[46] ASTM D638-14, "Standard test methods for Tensile properties of plastics," *American Society for Testing and Materials*, vol. 14, pp. 1–17, 2014.

[47] D. Mohana, D. Sreeramulu, and N. Ramesh, "Synthesis, characterization, and properties of epoxy filled Luffa cylindrica reinforced composites," *Materials Today: Proceedings*, vol. 5, no. 2, pp. 6518–6524, 2018.

[48] M. Z. Hassan, S. A. Roslan, S. M. Sapuan, and Z. A. Rasid, "Mercerization optimization of bamboo (Bambusa vulgaris) fiber-reinforced epoxy composite structures using a box—Behnken design," *Polymers*, vol. 12, pp. 1–19, 2020.

[49] D. Croccolo, M. De Agostinis, S. Fini et al., "Mechanical characteristics of two environmentally friendly resins reinforced with flax fibers," *Journal of Mechanical Engineering*, vol. 61, pp. 227–236, 2015.

[50] N. R. Sikame Tagne, T. E. Mbou, O. Harzallah et al., "Physicochemical and mechanical characterization of Raffia vinifera pith," *Advances in Materials Science and Engineering*, vol. 2020, 2020.

[51] ASTM D790-03, "Standard test methods for flexural properties of unreinforced and reinforced plastics and electrical insulating materials," *American Society for Testing and Materials*, pp. 1–11, 2003.

[52] A. K. Mehra, R. Saini, and A. Kumar, "The effect of fibre contents on mechanical and moisture absorption properties of gourd sponge/coir fibre reinforced epoxy hybrid composites," *Composites Communications*, vol. 25, pp. 1–8, 2021.

[53] A. Angioloni and C. Collar, "Promoting dough viscoelastic structure in composite cereal matrices by high hydrostatic pressure," *Journal of Food Engineering*, vol. 111, no. 4, pp. 598–605, 2012.

[54] C. L. Petzhold, R. D. A. Delucis, W. Luiz, and E. Magalh, "Forest-based resources as fillers in biobased polyurethane foams," *Journal of Applied Polymer Science*, vol. 45684, pp. 1–7, 2017.

[55] I. S. Santos, B. L. Nascimento, R. H. Marino, E. M. Sussuchi, M. P. Matos, and S. Griza, "Influence of drying heat treatments on the mechanical behavior and physico-chemical properties of mycelial biocomposite," *Composites Part B: Engineering*, vol. 217, p. 108870, 2021.

[56] M. Maache, A. Bezazi, S. Amroune, F. Scarpa, and A. Dufresne, "Characterization of a novel natural cellulosic fiber from Juncus effusus L," *Carbohydrate Polymers*, vol. 171, pp. 163–172, 2017.

[57] A. Roy, S. Chakraborty, S. P. Kundu, R. K. Basak, S. Basu Majumder, and B. Adhikari, "Improvement in mechanical properties of jute fibres through mild alkali treatment as demonstrated by utilisation of the Weibull distribution model," *Bioresource Technology*, vol. 107, pp. 222–228, 2012.

[58] J. F. Barbosa, R. Carlos, S. Freire, J. A. F. O. Correia, A. M. P. De Jesus, and R. A. B. Calc, "Analysis of the fatigue life estimators of the materials using small samples," *Journal of Strain Analysis*, vol. 53, pp. 1–12, 2018.

[59] D. Djeghader and B. Redjel, "Effect of water absorption on the Weibull distribution of fatigue test in jute-reinforced polyester composite materials," *Advanced Composites Letters*, vol. 28, pp. 1–11, 2019.

[60] K. Naresh, K. Shankar, and R. Velmurugan, "Reliability analysis of tensile strengths using Weibull distribution in glass/

epoxy and carbon/epoxy composites," *Composites Part B: Engineering*, vol. 133, pp. 1–38, 2017.

[61] S. Navaneethakrishnan, V. Sivabharathi, and S. Ashokraj, "Weibull distribution analysis of roselle and coconut-shell reinforced vinylester composites," *Australian Journal of Mechanical Engineering*, vol. 19, no. 4, pp. 457–466, 2021.

[62] B. Redjel, A. Remadnia, and M. Chaplain, "Utilisation du modèle probabiliste de Weibull à la caractérisation de l'aspect aléatoire de la rupture en traction de panneaux en bois à lamelles orientées," *23eme Congrès Français de Mécanique*, pp. 1–10, 2017, 39/41 rue Louis Blanc-92400 Courbevoie.

[63] S. Achouri and B. Redjel, "Experimental study and probabilistic analysis of the tensile fracture behavior of glass-perlon-acrylic reinforce," *Reviews Science Technology, Synthèse*, vol. 76, pp. 59–76, 2014.

[64] B. Issasfa, T. Benmansour, I. Pprime, U. De Poitiers, and B. Marie, "Experimental study of mechanical behaviour of renewable fibre reinforced composite materials type (Cynara Cardunculus L/polyester)," *Journal of Composites and Advanced Materials*, vol. 30, no. 1, pp. 1–8, 2020.

[65] R. H. Doremus, "Fracture statistics: a comparison of the normal, Weibull, and type I extreme value distributions," *Journal of Applied Physics*, vol. 193, no. 1983, pp. 193–198, 2009.

[66] M. Tiryakioğlu, D. Hudak, and G. Ökten, "On evaluating Weibull fits to mechanical testing data department of engineering," *Materials Science and Engineering*, vol. 527, pp. 397–399, 2009.

[67] I. Miraoui and H. Hassis, "Mechanical model for vegetal fibers-reinforced composite materials," *Physics Procedia*, vol. 25, pp. 130–136, 2012.

[68] E. Osoka, "A modified Halpin–Tsai model for estimating the modulus of natural fiber a modified Halpin–Tsai model for estimating the modulus of natural fiber reinforced composites," *International Journal of Engineering Science*, vol. 7, no. 5, pp. 63–70, 2018.

[69] S. Tido Tiwa, K. Bilba, R. P. de Oliveira Santos, C. Onésippe-Potiron, H. Savastano Junior, and M. A. Arsène, "Nanocellulose-based membrane as a potential material for high performance biodegradable aerosol respirators for SARS-CoV-2 prevention: a review," *Cellulose*, vol. 29, pp. 8001–8024, 2022, 0123456789.

[70] K. L. Pickering, M. G. A. Efendy, T. M. Le, and A. Efendy, "A review of recent developments in natural fibre composites and their mechanical performance," *Composites Part A: Applied Science and Manufacturing*, vol. 83, pp. 1–20, 2015.

[71] N. A. Ramlee, M. Jawaida, E. S. Zainudin, and S. A. K. Yamani, "Tensile, physical and morphological properties of oil palm empty fruit bunch/sugarcane bagasse fibre reinforced phenolic hybrid composites," *Journal of Materials Research and Technology*, vol. 8, pp. 1–9, 2019.

[72] N. S. Nor Arman, R. S. Chen, and S. Ahmad, "Review of state-of-the-art studies on the water absorption capacity of agricultural fiber-reinforced polymer composites for sustainable construction," *Construction and Building Materials*, vol. 302, p. 124174, 2021, July, Elsevier Ltd.

[73] A. Gupta, A. Kumar, A. Patnaik, and S. Biswas, "Effect of different parameters on mechanical and erosion wear behavior of bamboo fiber reinforced epoxy composites," *International Journal of Polymer Science*, vol. 2011, p. 11, 2011.

[74] M. Habibi, E. Ruiz, G. Lebrun, and L. Laperriere, "Effect of surface density and fiber length on the porosity and permeability of nonwoven flax reinforcement," *Textile Research Journal*, vol. 88, pp. 1–12, 2017.

[75] E. M. Tiaya, P. W. H. Mejouyo, P. A. N. Ewane, C. Damfeu, P. Meukam, and E. Njeugna, "Effect of particle sizes on physical, thermal and mechanical with raffia vinifera cork and Bambusa vulgaris," *Polymer Bulletin*, pp. 1–21, 2023, 0123456789.

[76] T. T. Stanislas, G. C. Komadja, O. F. Ngasoh et al., "Performance and durability of cellulose pulp-reinforced extruded earth-based composites," *Arabian Journal for Science and Engineering*, vol. 46, no. 11, pp. 11153–11164, 2021.

[77] T. T. Stanislas, J. F. Tendo, R. S. Teixeira et al., "Effect of cellulose pulp fibres on the physical, mechanical, and thermal performance of extruded earth-based materials," *Journal of Building Engineering*, vol. 39, pp. 1–12, 2021.

[78] G. Das and S. Biswas, "Effect of fiber parameters on physical, mechanical and water absorption behaviour of coir fiber-epoxy composites," *Journal of Reinforced Plastics and Composites*, vol. 35, no. 8, pp. 628–637, 2016.

[79] S. Pujari, P. A. Ramakrishna, and K. Tbalarampadal, "Comparison of ANN and regression analysis for predicting the water absorption behaviour of jute and banana fiber reinforced epoxy composites," *Materials Today: Proceedings*, vol. 4, pp. 1626–1633, 2017.

[80] O. O. Daramola, A. Adediran, B. O. Adewuyi, and O. Adewole, "Mechanical properties and water absorption behaviour of treated pineapple leaf fibre reinforced polyester matrix composites," *Leonardo Journal of Sciences*, vol. 30, no. 30, pp. 15–30, 2017.

[81] B. Stalin and R. Ramkumar, "Mechanical properties of bauhinia racemosa fiber reinforced with polymer composites," *International Journal of Applied Engineering Research*, vol. 10, no. 51, pp. 701–705, 2015.

[82] A. N. Anyakora and O. K. Abubakre, "Effect of fibre loading and treatment on porosity and water absorption correlated with tensile behaviour of oil palm empty fruit bunch fibre reinforced composites," *Advanced Materials Research*, vol. 6, no. 4, pp. 329–341, 2018.

[83] Z. Kamble, B. K. Behera, T. Kimura, and I. Haruhiro, "Development and characterization of thermoset nanocomposites reinforced with cotton fibres recovered from textile waste," *Journal of Industrial Textiles*, vol. 51, pp. 1–27, 2020.

[84] Y. A. El-shekeil, S. M. Sapuan, K. Abdan, and E. S. Zainudin, "Influence of fiber content on the mechanical and thermal properties of Kenaf fiber reinforced thermoplastic polyurethane composites," *Materials and Design*, vol. 40, pp. 299–303, 2012.

[85] R. Wirawan, S. M. Sapuan, R. Yunus, and K. Abdan, "Properties of sugarcane bagasse/poly(vinyl chloride) composites after various treatments," *Journal of Composite Materials*, vol. 45, no. 16, pp. 1667–1674, 2010.

[86] S. Ozturk, "Effect of fiber loading on the mechanical properties of Kenaf and fiberfrax fiber-reinforced phenol-formaldehyde composites," *Journal of Composite Materials*, vol. 44, no. 19, pp. 2265–2288, 2010.

[87] M. Jacob, S. Thomas, and K. T. Varughese, "Mechanical properties of sisal/oil palm hybrid fiber reinforced natural rubber composites," *Composites Science and Technology*, vol. 64, no. 7–8, pp. 955–965, 2004.

[88] S. Joseph, M. S. Sreekala, Z. Oommen, P. Koshy, and S. Thomas, "A comparison of the mechanical properties of phenol formaldehyde composites reinforced with banana

fibres and glass fibres," *Composites Science and Technology*, vol. 62, no. 14, pp. 1857–1868, 2002.

[89] T. P. Sathishkumar, P. Navaneethakrishnan, and S. Shankar, "Tensile and flexural properties of snake grass natural fiber reinforced isophthallic polyester composites," *Composites Science and Technology*, vol. 72, no. 10, pp. 1183–1190, 2012.

[90] T. Haghighatnia, A. Abbasian, and J. Morshedian, "Hemp fiber reinforced thermoplastic polyurethane composite: an investigation in mechanical properties," *Industrial Crops and Products*, vol. 108, pp. 853–863, 2017.

[91] M. S. Islam, K. L. Pickering, and N. J. Foreman, "Influence of alkali fiber treatment and fiber processing on the mechanical properties of hemp/epoxy composites influence of alkali fiber treatment and fiber processing on the mechanical properties of hemp/epoxy composites," *Journal of Applied Polymer Science*, vol. 119, pp. 3696–3707, 2009.

[92] J. Datta, "Effect of kenaf fibre modification on morphology and mechanical properties of thermoplastic polyurethane materials," *Industrial Crops and Products*, vol. 74, pp. 566–576, 2015.

[93] A. K. Sylwia Członka and A. S. ˛akowska, "Coir fibers treated with henna as a potential reinforcing filler in the synthesis of polyurethane composites," *Materials*, vol. 14, pp. 1–16, 2021.

[94] Y. Du, N. Yan, and M. T. Kortschot, *The Use of Ramie Fibers as Reinforcements in Composites*, pp. 104–137, Elsevier Ltd, Toronto, Canada, 2014.

[95] K. Mylsamy and I. Rajendran, "Influence of alkali treatment and fibre length on mechanical properties of short Agave fibre reinforced epoxy composites," *Materials and Design*, vol. 32, no. 8–9, pp. 4629–4640, 2011.

[96] K. S. Kumar, I. Siva, P. Jeyaraj, J. T. W. Jappes, S. C. Amico, and N. Rajini, "Synergy of fiber length and content on free vibration and damping behavior of natural fiber reinforced polyester composite beams," *Journal of Materials*, vol. 56, p. 386, 2014.

[97] S. K. Ray, K. K. Singh, and M. T. A. Ansari, "Effect of small ply angle variation in tensile and compressive strength of woven GFRP composite: application of two parameter Weibull distribution," *Materials Today: Proceedings*, vol. 33, pp. 5295–5300, 2020.

[98] M. Quintero-Davila, S. N. Monteiro, and d. H. A. Colorado, "Composites of Portland cement and fibers of Guadua angustifolia Kunth from Colombia," *Journal of Composite Materials*, vol. 53, pp. 2–10, 2018.

[99] E. Trujillo, M. Moesen, L. Osorio, A. W. Van Vuure, J. Ivens, and I. Verpoest, "Bamboo fibres for reinforcement in composite materials: strength Weibull analysis," *Composites Part A: Applied Science and Manufacturing*, vol. 61, pp. 115–125, 2014.

[100] M. M. A. Sayeed and A. Paharia, "Optimisation of the surface treatment of jute fibres for natural fibre reinforced polymer composites using Weibull analysis," *Journal of the Textile Institute*, vol. 110, pp. 1–8, 2019.

[101] P. V. Joseph, G. Mathew, K. Joseph, S. Thomas, and P. Pradeep, "Mechanical properties of short sisal fiber-reinforced polypropylene composites: comparison of experimental data with theoretical predictions," *Journal of Applied Polymer Science*, vol. 88, pp. 602–611, 2003.

[102] F. K. Sodoke, L. Toubal, and L. Laperrière, "Hygrothermal effects on fatigue behavior of quasi-isotropic flax/epoxy composites using principal component analysis," *Journal of Materials Science*, vol. 51, no. 24, pp. 10793–10805, 2016.